Hydrothermally Altered Rock and Hot-Spring Deposits at Yellowstone National Park—Characterized Using Airborne Visible- and Infrared-Spectroscopy Data

By K. Eric Livo, Fred A. Kruse , Roger N. Clark, Raymond F. Kokaly, and W.C. Shanks, III

Chapter O *of*
Integrated Geoscience Studies in the Greater Yellowstone Area—Volcanic, Tectonic, and Hydrothermal Processes in the Yellowstone Geoecosystem
Edited by Lisa A. Morgan

Professional Paper 1717

U.S. Department of the Interior
U.S. Geological Survey

Contents

Figures

Hydrothermally Altered Rock and Hot-Spring Deposits at Yellowstone National Park—Characterized Using Airborne Visible- and Infrared-Spectroscopy Data

By K. Eric Livo,[1] Fred A. Kruse ,[2] Roger N. Clark,[1] Raymond F. Kokaly,[1] and W.C. Shanks, III[1]

Abstract

The hydrothermal system in Yellowstone National Park has created altered rock and hot-spring deposits that were mapped using AVIRIS (airborne visible and infrared imaging spectrometer) data. The mapped minerals are indicative of the geologic processes and environments that controlled their formation. Ongoing volcanic activity is expressed at the surface by geothermal features, earthquakes, and geologically recent caldera formation. Precipitated minerals such as siliceous sinter and travertine on the surface are derived from chloride-rich alkaline solutions that are leaching silica and calcite from the underlying country rock. Siliceous sinter and montmorillonite are associated with hydrothermal systems abundant in hot water, whereas kaolinite and alunite are associated with acidic-vapor-dominated hydrothermal systems.

Introduction

Remotely sensed data are used to map hydrothermally altered rock and hot-spring deposits in Yellowstone National Park (the Park). The airborne imaging-spectroscopy data contain spectra of reflected light that record absorption features that are unique to the surface materials from which sunlight is reflected. Analysis of these features permits identification of the mineralogy of some surface soils and bedrock lithologies.

Hydrothermal-water chemistry and bedrock lithologies can be inferred from the types of minerals on the land surface. Researchers have extensively studied water chemistry in Yellowstone National Park and the associated altered minerals that form within the hydrothermal cells. This report links the observed altered rock, identified from imaging-spectroscopy data, with the underlying geological processes, and it associates mineral trends with fracture systems.

[1]U.S. Geological Survey, Denver Box 25046, M.S. 973, Denver Federal Center, Denver CO 80225.

[2]Horizon GeoImaging, LLC, 4845 Pearl East Circle, Suite 101, Boulder, CO 80301.

Methods

Remotely sensed data were collected using NASA's Jet Propulsion Laboratory airborne visible and infrared imaging spectrometer (AVIRIS) in the late summer of 1996 and fall of 1998. Data were collected at a pixel-spatial resolution of 20 m in most of the Park (in 1996) and at a pixel-spatial resolution of 2×6 m at selected sites (in 1998). Both data sets have 224 continuous spectral channels ranging from 0.4 to 2.5 micrometers (μm). Minerals were spectrally identified using the U.S. Geological Survey (USGS) Tetracorder program (Clark and others, 1990, 1991, 2003; Clark, Swayze, and Gallagher, 1993; Clark and Swayze, 1995; Rockwell and others, 1999) and methods developed by Analytical Imaging and Geophysics (AIG) (Kruse and others, 1996; Boardman, 1997, 1998; Kruse, 1998, 1999). USGS processing utilized a custom goodness-of-fit spectral-analysis routine, whereas AIG processing characterized "pure" spectral end-members (Kruse and others, 1993; Kruse, 1998, 1999) using the Environment for Visualizing Images (ENVI) software (Research Systems, Inc., Boulder, Colo.). Both analysis techniques use spectral libraries for initial material identification. Hyperspectral-mapping methods were then used to determine the occurrence and abundance of specific materials. These data were then field-checked to ensure correct identification.

Spectral Identification of Minerals

Spectral identification of minerals is accomplished by using diagnostic absorption features within the measured light spectrum. Every pixel in the image has a measured spectrum that can be visually or mathematically analyzed, comparing the pixel-spectral features against known mineral-spectral features. A variety of techniques exist for this analysis. We used the USGS Tetracorder method, in which the spectral features of an image pixel are compared to data from a mineral-spectral library, and we also used the AIG ENVI end-member method to identify unique spectral end-members.

USGS Methods

AVIRIS data were converted from radiance to reflectance and then calibrated to absolute reflectance relative to ground. This two-step process is described in Clark, Swayze, Heidebrecht, and others (1993). The first step uses the atmospheric-removal algorithm (ATREM) (Gao and others, 1997) to remove atmospheric effects of solar irradiance, atmospheric absorption, and atmospheric scattering and then converts the data from radiance to reflectance. In the second step, residual atmospheric absorptions were removed by calibrating the data against field data measured with a hand-held spectrometer at a calibration site.

Spectral-feature analysis was then used to identify minerals in the image. The USGS Tetracorder program (Clark and others, 2003) was used for initial processing and identification. This program tests band-absorption features from the image-pixel spectra against known mineral-absorption features from the USGS mineral library using a goodness-of-fit algorithm. Multiple (continuum-removed) absorption features for each spectrum are used concurrently to generate a weighted average for spectral goodness-of-fit, band depth, and fit × depth. Defined thresholds for each value must be exceeded. The mineral-library spectrum with the highest goodness-of-fit value is selected for initial identification for each pixel. Image pixels containing abundant vegetation are masked. Visual analysis and iterative processes that vary internal tetracorder parameters and add new mineral spectra to the spectral library are used to create the final mineral identifications (the mineral maps).

Analytical Imaging and Geophysics Method

Spectral-feature analysis using the AIG method began with calibrated AVIRIS data derived from ATREM. Artifacts were removed using the AIG program "Effort," which performs a statistical running average. No field calibration was performed. ENVI software was used to derive end-member spectra using standard minimum-noise (statistical) derivatives. Mineral identification of the end-member spectra used mineral-library-classification routines within ENVI and visual interpretation of the end-member spectra.

Geologic Structure, Volcanic History, and Geologic Setting

The Yellowstone National Park region was the locus of three large caldera-forming volcanic eruptions during the last 2.1 million years. Widespread airborne volcanic ash and lava flows cover much of the present land surface from these and later eruptions. Volcanic activity is ongoing, and heat flow is 30 times greater than the continental average (Smith and Braile, 1993). The volcanism is associated with intensive earthquake activity (Smith and Braile, 1993) that drives the geothermal system; it continually opens and reopens radial- and concentric-fracture systems, thus maintaining local fluid pathways.

One hypothesis is that the volcanic activity is a result of the North American crustal plate overriding a hot-spot mantle plume. The volcanic lavas and ash deposits overlie crustal sedimentary, igneous, and metamorphic rocks. Two important rock types that influence the mineral-alteration assemblages in the region are the widespread quartz-rich rhyolite flows that underlie many of the geyser basins and the limestone that underlies the terraces at Mammoth Hot Springs.

Alteration Minerals

Figure 1 (from Mosier and others, 1986) shows a cross-section model (Creede system) illustrating the alteration pattern that is typical for acid-sulfate hydrothermal-vein systems such as those in Yellowstone National Park. This model illustrates the fluid channelways that allow ascending hot water to react with the wallrock, altering the existing minerals. Quartz, adularia, illite, and sulfides, with or without kaolinite, are formed at depth, whereas quartz, kaolinite, and alunite are formed near the surface. White and others (1975) drilled and cored several geyser basins and identified a similar distribution of minerals within the acid-sulfate system at Porcelain Terrace in Norris Geyser Basin. At depths of 600 to 1,000 ft, mixed-layer illite-montmorillonite with pyrite was present; from 200 to 600 ft, kaolinite, sparse montmorillonite, cristobalite, chalcedony, goethite, and sanidine were present; and from the surface to a depth of 200 ft, alunite, kaolinite, cristobalite, and sanidine were present.

Hydrothermal Waters

Water chemistry is a controlling factor in determining the species of mineral alteration. White and others (1988) extensively drilled and cored Norris, Lower, and Upper Geyser Basins. They determined water-chemistry changes with depth, and they associated mineral-alteration species with water chemistry. They identified four types of water. Type-1 water is of neutral pH and is chloride-silica rich; it has altered the mafic minerals in rhyolite country rock to goethite, hematite, and chalcedony and has changed plagioclase to siliceous sinter and montmorillonite. Type-2 water is formed from vapor-dominated gas and has less chloride than the other water types. Near the surface, type-2 water is acidified by oxidation of hydrogen sulfide; it is then recirculated and reheated within 100 ft of the surface. Type-2 water bleaches the surrounding country rock, leaches ferric oxides, and creates montmorillonite, illite, and chlorite. Type-3 water is acid-chloride-sulfate rich and

is generated by restricted flow of neutral pH, chloride-silica-rich water that combines with sulfur and rain and snowmelt surface water. Type-3 water bleaches the country rock, leaching all ferric oxides. Type-4 water is acid-sulfate rich, low in chloride, and is generated above a boiling water table where steam combines with hydrogen sulfide gas to yield restricted, hot, low-pH water. Type-4 water bleaches the country rock, leaches ferric oxides, and alters potassium feldspar and sanidine to kaolinite, opal, and cristobalite. Type-4 water forms mixed-layer clay minerals—montmorillonite is dominant at temperatures lower than 198°C; mixed-layer montmorillonite-illite is dominant between 198°C and 238°C; and illite is dominant at temperatures higher than 238°C (White and others, 1988).

Chloride-rich siliceous sinter deposited by type-1 water is widespread in Upper and Lower Geyser Basins, on the basin floor at Norris Geyser Basin, and in the Hayden River valley. Acid-sulfate deposits are common at Roaring Mountain, in the Grand Canyon of the Yellowstone River, and at higher elevations at Norris Geyser Basin. The near-surface alunite environment was characterized by White and others (1988) and Thompson (1991) as containing chalcedony and porous opaline sinter, sulfur, and cristobalite that formed from decomposed rhyolite—all associated with sulfurous gases and aqueous vapors emitted from ground fissures.

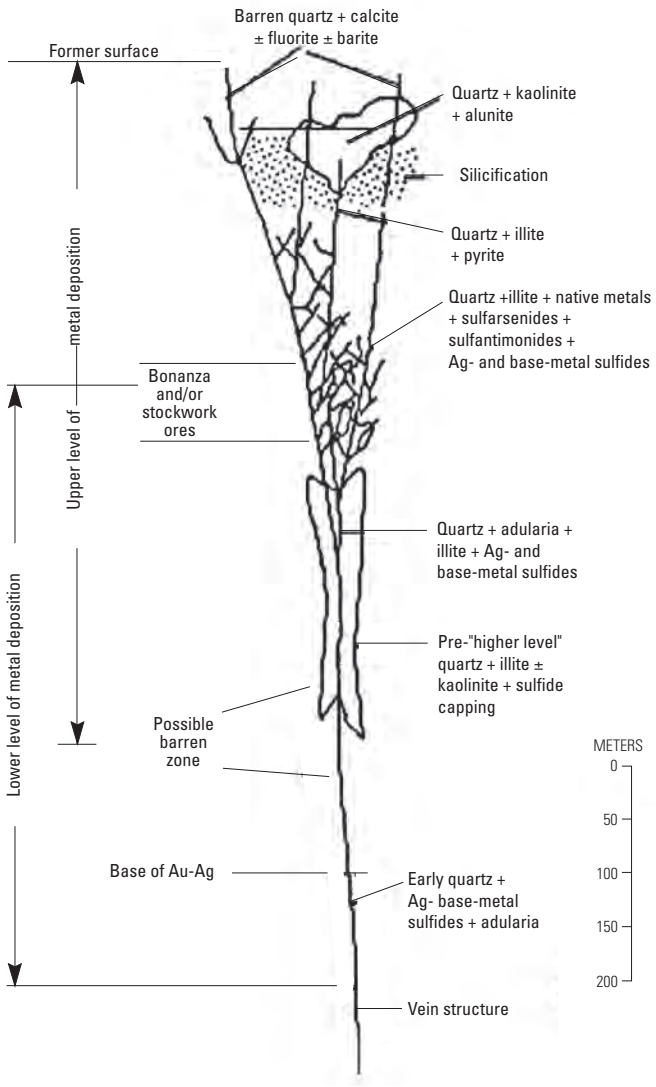

Figure 1. Schematic cross section of USGS mineral deposit model 25b. This interpretive model for the Creede caldera system exhibits the alteration pattern typical for acid-sulfate systems (from Mosier and others, 1986).

Hyperspectral Remote Sensing

The AVIRIS imaging-spectrometry data contains 224 channels measured from the edge of the ultraviolet through the visible and into the near-infrared wavelengths of light. Each data channel (wavelength interval or band) forms an image of the Earth's surface as an array of pixels, with all data channels coregistered to each other. Each pixel (geographic location in the image) contains a spectrum formed from the 224 channels of data.

Spectral identification of minerals uses diagnostic absorption features within the measured light spectrum. Absorption features have band-center wavelengths, band depths, and band shapes that can be used to characterize every mineral. When these features are unique, they identify specific minerals, such as kaolinite, montmorillonite, and alunite. When these features are shared by several minerals (as in illite, sericite, and muscovite) or mineral combinations, they differentiate a spectral group of minerals. These absorption features are the result of the way molecular bands interact with incident light within the mineral. They indicate compositional differences in the minerals, but not structural differences.

Spectral abundance of a mineral may be qualitatively characterized using the intensity of its absorption-feature band depth. Quantitative measurements require knowledge of mineral-grain sizes, exact mineral-mixture proportions, and mineral chemical compositions and ion substitutions, all of which must be characterized in the laboratory.

Examples of spectra for several minerals in the Yellowstone hot-spring environments are shown in figures 2 and 3. Figure 2 shows the spectra for clay minerals, calcite, alunite, and siliceous sinter. The unique absorption features of interest generally are in the 2.2- to 2.4-μm-wavelength region. Siliceous sinter, as used here, is a spectral group of SiO_2 minerals including opal, chalcedony, and cristobalite derived from hydrothermal fluids and (or) the decomposition of rhyolite. The identification of these minerals uses a hydration-absorption feature that is present in some silica at the 2.2- to 2.4-μm-wavelength region. Quartz does not have this absorption feature; therefore it is not readily identified within AVIRIS wavelengths. Figure 3 shows the spectra for iron oxide (hematite), iron hydroxide (goethite), and iron sulfate (jarosite). Shifts in the absorption-feature minima of these

minerals in the 0.5- to 0.6-µm region are responsible for the colors of minerals as the eye sees them—yellow (jarosite), brown (goethite), and red (hematite). Other features used for identification are in the 0.42- and 0.9-µm wavelengths.

A partial sequence of the mineralization, identified by White and others (1975) and Keith and others (1978) using drill-core and water-chemistry studies, was spatially mapped using the imaging-spectroscopy data for surface exposures along the Firehole River (Upper, Midway, and Lower Geyser Basins), at Roaring Mountain, in the Grand Canyon of the Yellowstone River, and in parts of Norris Geyser Basin. The association of mineralization, identified by White and others (1975), with spectrally mapped areas of mineralization, links the geochemistry identified in past studies with our present results. Kaolinite and alunite were mapped at the tops of active hydrothermal systems and along the canyon rim of the Yellowstone River, whereas illite and montmorillonite were mapped on the lower walls of the canyon. Iron oxides were mapped in minor amounts throughout the Park, except for the Yellowstone canyon, where they are present in massive, complex combinations of hematite and goethite in association with the iron-sulfate mineral jarosite.

Mapping Results

The mapping results were verified; limited field-checking during a 2-week field excursion indicated very good agreement between the geology and the maps. The Upper, Lower, and Norris Geyser Basins, Mammoth Hot Springs, and the west end of the rim of the Grand Canyon of the Yellowstone River were examined in the field. The canyon walls and the northeast end of the Yellowstone Grand Canyon were not examined. The field verification included examination of hand-held samples and spectral field measurements using an ASD (analytical spectral devices) field spectrometer. Several dozen samples were brought to the laboratory for further spectral characterization. Results also were checked by examining spectra from the AVIRIS data over areas of known mineralization and over mineral locations identified through our mapping algorithms.

Several mineral groups were mapped, and specific minerals were identified. Kaolinite-family clay minerals are grouped, although minor spectral differences exist. The illite/sericite/muscovite spectral group is mapped as a general clay-mineral unit whose mineral members are spectrally indistinguishable and are referred to as illite. Two types of

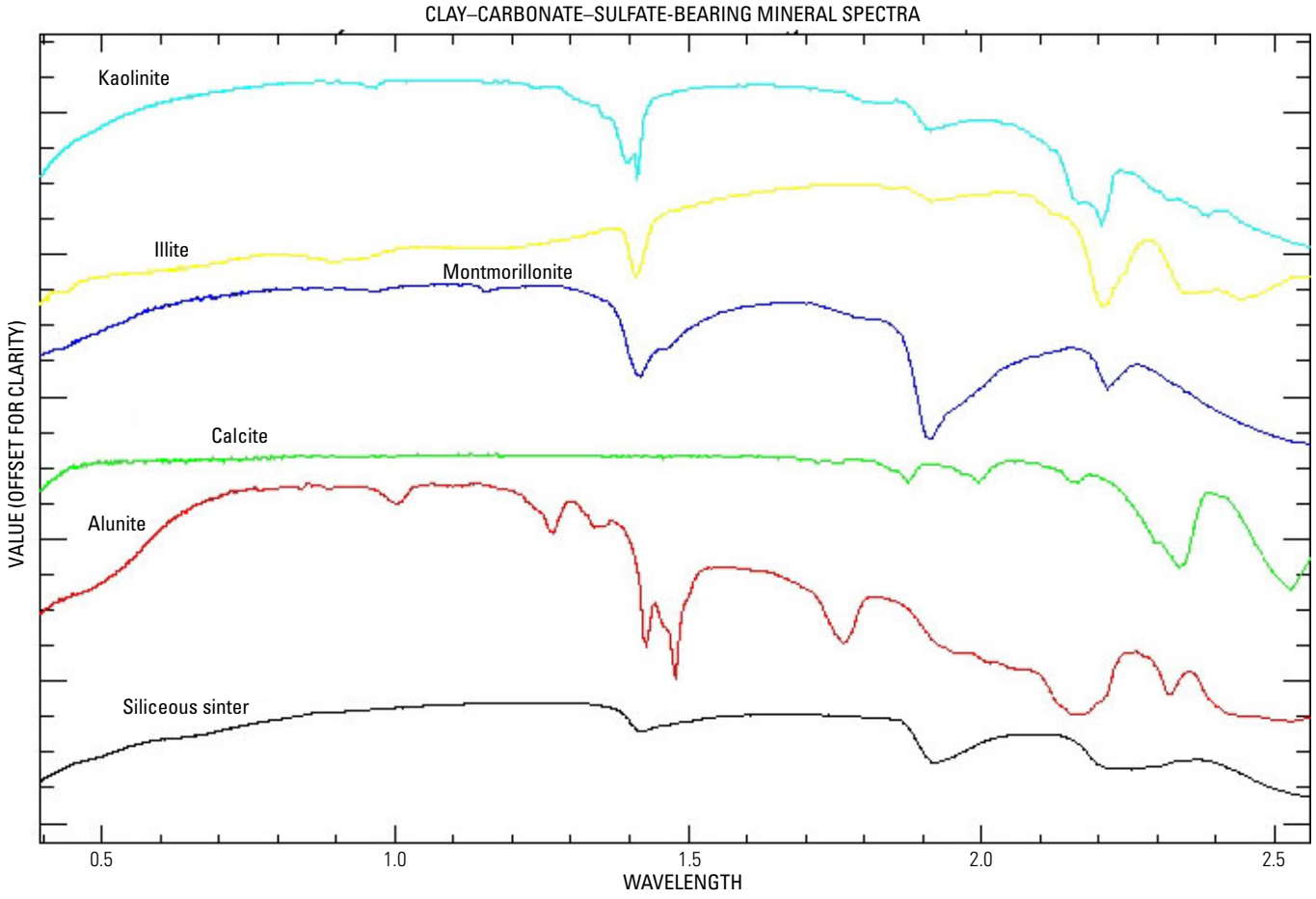

Figure 2. Mineral spectra for clay minerals, calcite, alunite, and siliceous sinter.

siliceous sinter were mapped—one is spectrally pure, and the other appears to be mixed with clay minerals. In this report, chalcedony, opaline sinter, and cristobalite are not spectrally separated; they are grouped as siliceous sinter.

Upper, Midway, and Lower Geyser Basins

Several large siliceous sinter deposits trend parallel to the Firehole River. These deposits generally are near the valley bottoms. They formed from neutral-pH chloride-rich hydrothermal fluids (White and others, 1975; Bargar and Beeson, 1985). Figures 4*A* and 4*B* provide an overview of hot-spring activity in the vicinity of the Firehole River. The deposits mapped, using the 1996, 20-m-pixel AVIRIS data, are characteristic of those in alkaline, active hot-spring environments and are consistent with the known mineralogy of the systems in Yellowstone National Park. The principal mineral adjacent to the Firehole River is hydrothermal silica, which has a characteristic spectral signature. Kaolinite, indicating more acidic water, also is present in some areas. Biological elements of the hot-spring systems also were mapped (principally, coloring of deposits and (or) thermal waters by thermophilic algae; see Kokaly and others, this volume). Chlorophyll-rich vegetation is shown in shades of red in figure 4*A* (false-color composite using AVIRIS wavelengths 0.85, 0.67, and 0.55 μm; colored red, green, and blue, respectively). In figure 4*A*, siliceous sinter deposits are colored white and dry grass and burnt areas are colored light green. Figure 4*B* (AVIRIS minerals map) provides an overview of the distribution of selected geologic materials; silica and kaolinite are colored green and red and show the locations of major geyser basins.

The Upper Geyser Basin sinter deposits (fig. 5; 1998, 6-m spatial-resolution image) are on a northwest linear trend (also seen at the bottom of fig. 6; 20-m resolution). The Midway Basin (sinter at the center of fig. 6) and Lower Geyser Basin (sinter at the top of fig. 6) sinter deposits appear to form a semicircular feature in the AVIRIS image. Generally, these deposits contain an inner zone of sinter mixed with minor amounts of clay minerals, whereas the outer regions are only sinter. Kaolinite deposits are scattered in and west of Old Faithful Geyser (bottom right sinter deposit with a semicircular boardwalk in fig. 5), east of Midway Geyser Basin (right center, fig. 6), and along a northeastward trend on the north side of Lower Geyser Basin (top, fig. 6). The presence of kaolinite, which is associated with acid-sulfate alteration, indicates the presence of local sulfur-rich fluids in basins that contain

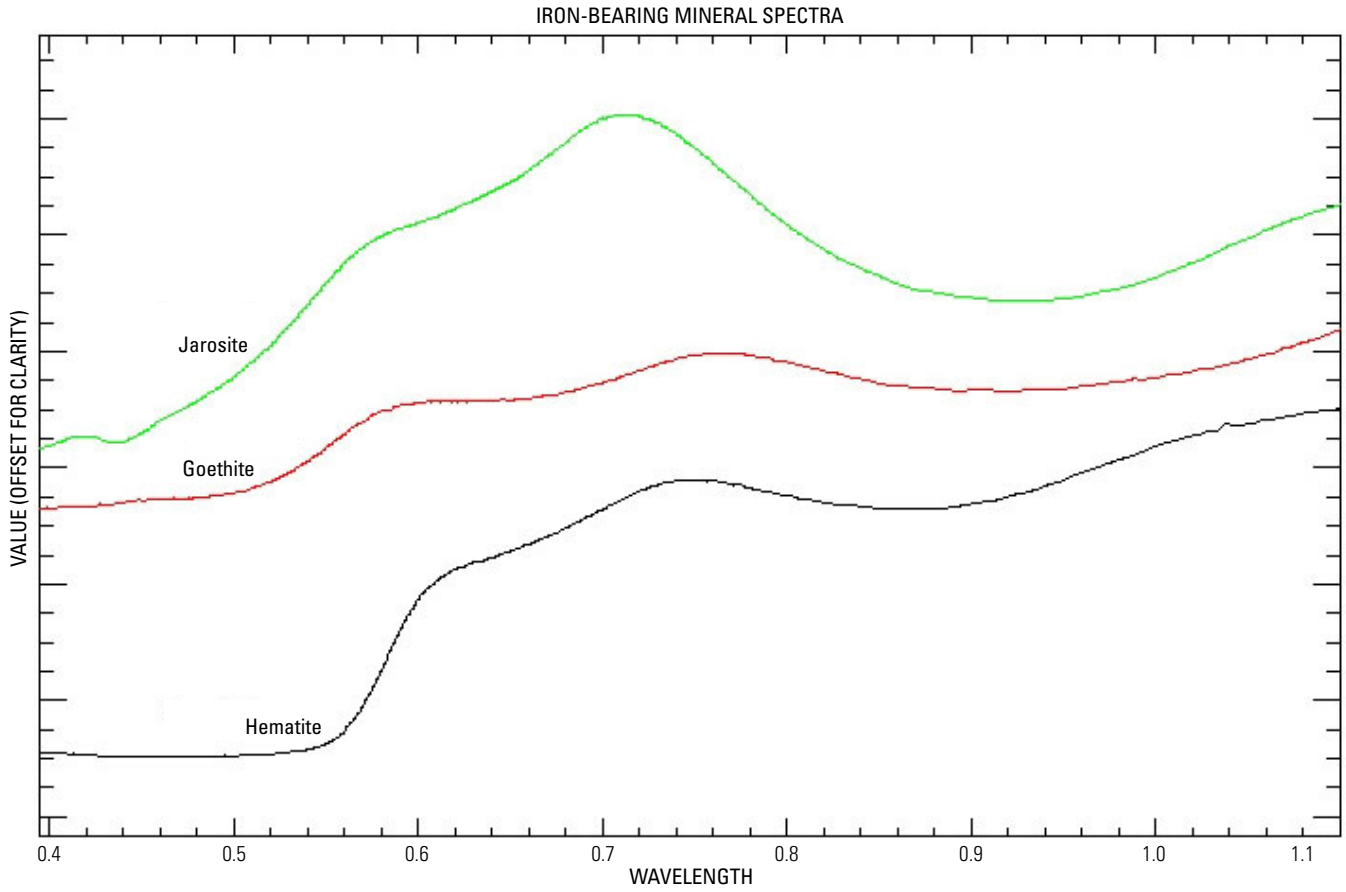

Figure 3. Mineral spectra for iron-bearing minerals.

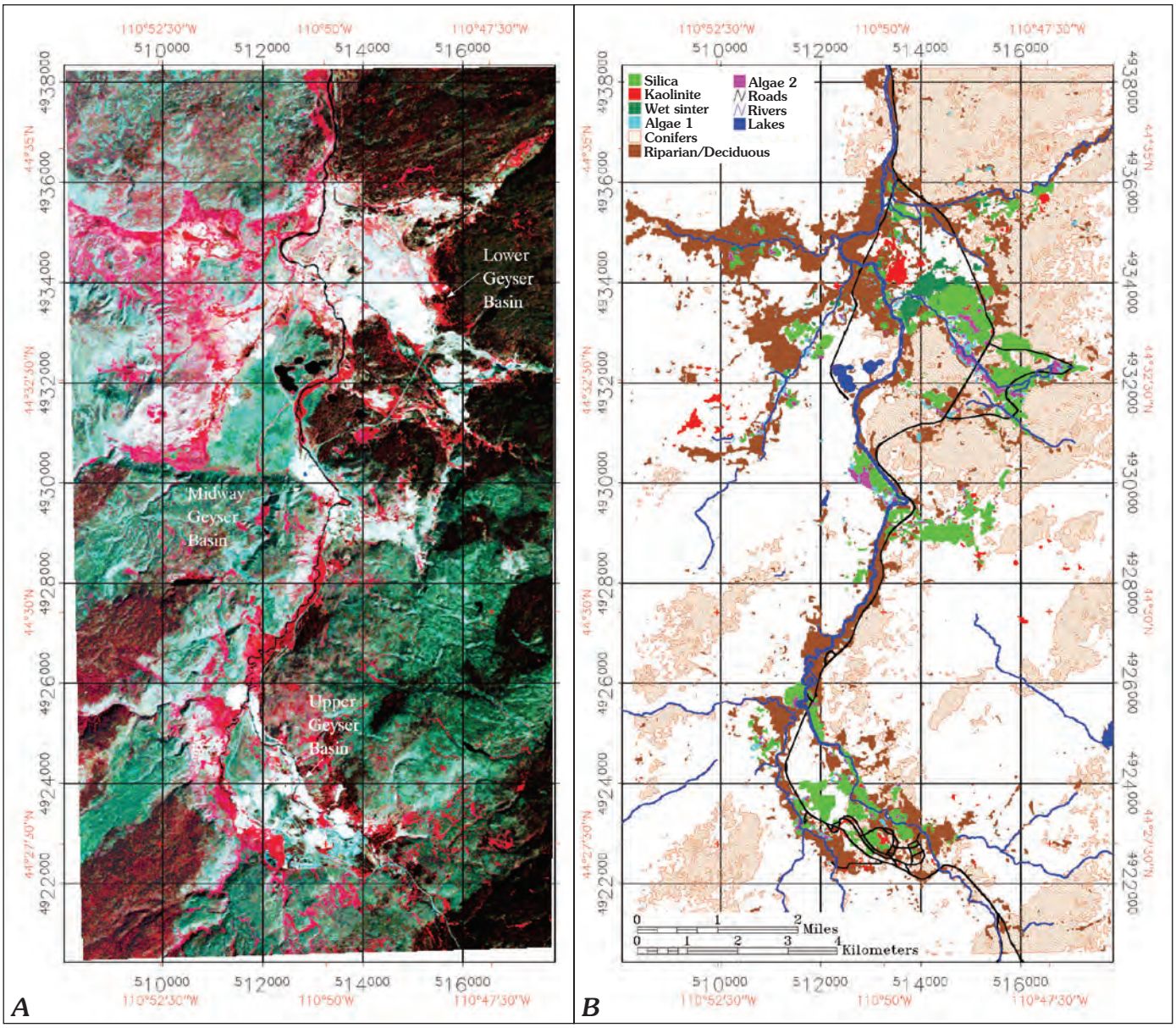

Figure 4. 1996 AVIRIS maps. *A,* false-color composite map. *B,* Derived map.

neutral-pH chloride-rich water. Wet soils are widespread in the Lower Geyser Basin; they are less common in the Upper Geyser Basin. These soils are in drainage channels that lead from hot-spring vents, as seen on the 6-m resolution (low altitude) image in figure 5. Figure 5 also shows the kaolinite in the Old Faithful Geyser sinter (noted above) very near to, or within, one of the discharge channels. A minor kaolinite anomaly also is present just west of the Old Faithful Inn in a slightly raised area at the south end of the northwestward linear trend of sinter deposits. Generally, kaolinite appears to be present in drier surroundings; it is not closely associated with wet soils.

The AIG- and USGS-derived maps (figs. 4, 5, and 6) identify and locate similar mineralogy. Although both methods use the same data, the processes are significantly different. AIG methods detect statistical spectral differences in the data, and then they identify the resulting "end-member" spectra in the entire data set. USGS Tetracorder processing is rules based and statistically identifies the mineralogy of each pixel, independent of any other pixel, using a matching mineral-spectral library.

Norris Geyser Basin

Norris Geyser Basin (lower center, fig. 7) contains a complex mix of mineral-alteration suites formed by ongoing fluctuations of the underlying hydrothermal-system water chemistry. It contains four siliceous-sinter centers in the basin lowland, an alunite center on a hill to the southwest, and kaolinite encircling the basin sides. Alunite and kaolinite

follow an apparent north-south linear trend on the west side of the basin. The large alunite center (Ragged Hills) is on the south end of this trend, and kaolinite and minor alunite are on the north end.

Stable isotopes of alunite collected at Ragged Hills and Roaring Mountain were studied by Pat Shanks (USGS) using hydroxyl and sulfate components. Sulfur-isotope values indicated that the alunite at Ragged Hills was derived from sulfate, that in turn, was derived from surficial oxidation of H_2S in steam. Alunite and kaolinite rimming the geyser basin may be indicative of changes in water chemistry from neutral-pH chloride-rich water in the basin to a low-pH vapor-dominated system on the topographically higher sides of the basin. The study concluded that, although the Norris Geyser Basin sulfur isotopes of alunite were similar to those of local geothermal H_2S, the sulfur isotopes of the Roaring Mountain alunite were significantly different. This may indicate that the Roaring Mountain alunite is much older than the Norris Geyser Basin alunite.

Roaring Mountain

Roaring Mountain (mid-upper left, fig. 7), just north of Norris Basin, is a large acid-sulfate system with a restricted, steam-heated vapor-dominated water supply. A region of alunite-rich ground mixed with kaolinite is surrounded by areas characterized by abundant kaolinite. Sparse siliceous sinter is present west of Roaring Mountain, near the road. A calcite center east of the main alunite deposit at Roaring Mountain was field-checked; the calcite is Paleozoic limestone.

Preliminary field examination in Norris Geyser Basin indicates that the siliceous sinter is in down-cut, eroded, lowland sites. Alunite-kaolinite-rich deposits are resistant to erosion and become topographic highs. An understanding of the time of formation of the alunite and kaolinite and the mineralization-formation depth is complicated by this erosional process. Siliceous sinter presently is being deposited. In the field, we observed deposition of new terrace deposits and deposition of sinter onto and around the wooden boardwalk.

Areas surrounding Norris Geyser Basin and Roaring Mountain contain significant mineral alteration. In figure 7, a large alteration center is at Elk Park. Elk Park (west of Norris Geyser Basin) contains a major center of kaolinite-alunite, which is bordered on the east by siliceous sinter.

Grand Canyon of the Yellowstone River

The Grand Canyon of the Yellowstone River allows a three-dimensional perspective of an acid-sulfate system in which sulfur-rich hydrothermal fluids have leached the surrounding country rock and converted feldspar minerals to clay minerals. The clay mineralogy is dependent on temperature and pressure (White and others, 1988); kaolinite is present near the surface, and mixed-layer illite-montmorillonite is forming at depth. Iron is leached from mafic minerals in this acidic (low pH) environment and then combines with sulfur to form pyrite. Pyrite weathers to jarosite, which has been spectrally identified in the canyon. Alunite with kaolinite forms near the surface. Adjacent to this acid-sulfate hydrothermal system, chloride-rich alkaline water deposits siliceous sinter at the surface. Figure 8*A* shows the locations of mapped clay minerals, siliceous sinter, and alunite. Figure 8*B* shows the locations of mapped iron-bearing oxide, hydroxide, and sulfate.

In the northeastern third of the canyon, alteration minerals were mapped primarily on the north side of the canyon. Kaolinite was mapped along the canyon rim and down to the canyon bottom. Alunite is present with kaolinite; alunite and kaolinite centers are near the rim top at Sulphur Creek, and small exposures are on the north wall and near the canyon bottom. Kaolinite was differentiated into two spectral types: a "spectrally pure kaolinite" (colored orange in fig. 8*A*) and mixed kaolinite with other clay minerals (probably sericite or illite) (colored magenta in fig. 8*A)*. The "spectrally pure kaolinite" and alunite are associated with goethite, whereas the mixed kaolinite is associated with jarosite and hematite (compare figs. 8*A* and 8*B*). The distributions of jarosite, hematite, and mixed kaolinite indicate the presence of strongly acidic conditions near the canyon rim (possibly quartz-sericite-pyrite alteration), whereas the distributions of goethite and alunite indicate the presence of a milder acidic environment north of the rim. Hot-spring deposits of siliceous sinter with montmorillonite are evident along Sulphur Creek, near the canyon bottom, and on the south rim at Moss Creek; montmorillonite is present on the canyon bottom extending to the northeast edge of the image.

In the southwestern third of the canyon, kaolinite was mapped along the rim and on the canyon walls. "Spectrally pure kaolinite" in figure 8*A* is along the rim and is associated with jarosite along the upper canyon slopes. Kaolinite, mixed with other clay minerals and alunite, is on the lower slopes and is associated with goethite and goethite-jarosite mixtures. Hematite is in two centers; it is associated with both spectral classes of kaolinite. Illite is present in the lower half of the canyon, and montmorillonite is at the bottom; both minerals are associated with goethite.

Hot springs just south of the canyon have formed a small alunite-kaolinite-goethite center, which is surrounded by siliceous sinter. The sinter includes kaolinite and lesser montmorillonite, indicating a change in local water composition (at least at the surface) from the water that mineralogically altered the canyon terrain. Sulphur Springs and Violet Springs, farther south in the Hayden valley, contain siliceous-sinter cores surrounded by montmorillonite and lesser kaolinite.

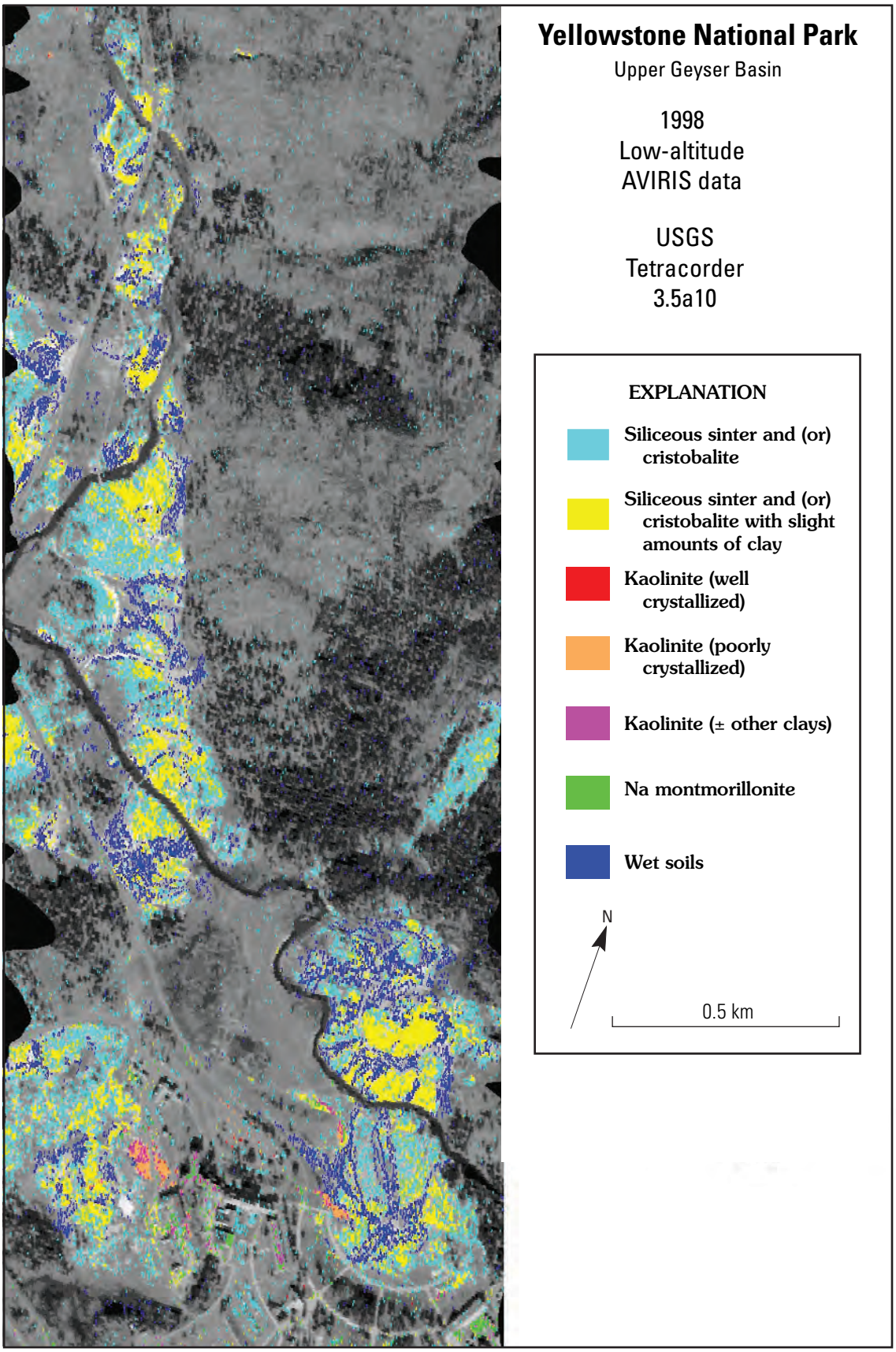

Figure 5. Mineral map of Upper Geyser Basin.

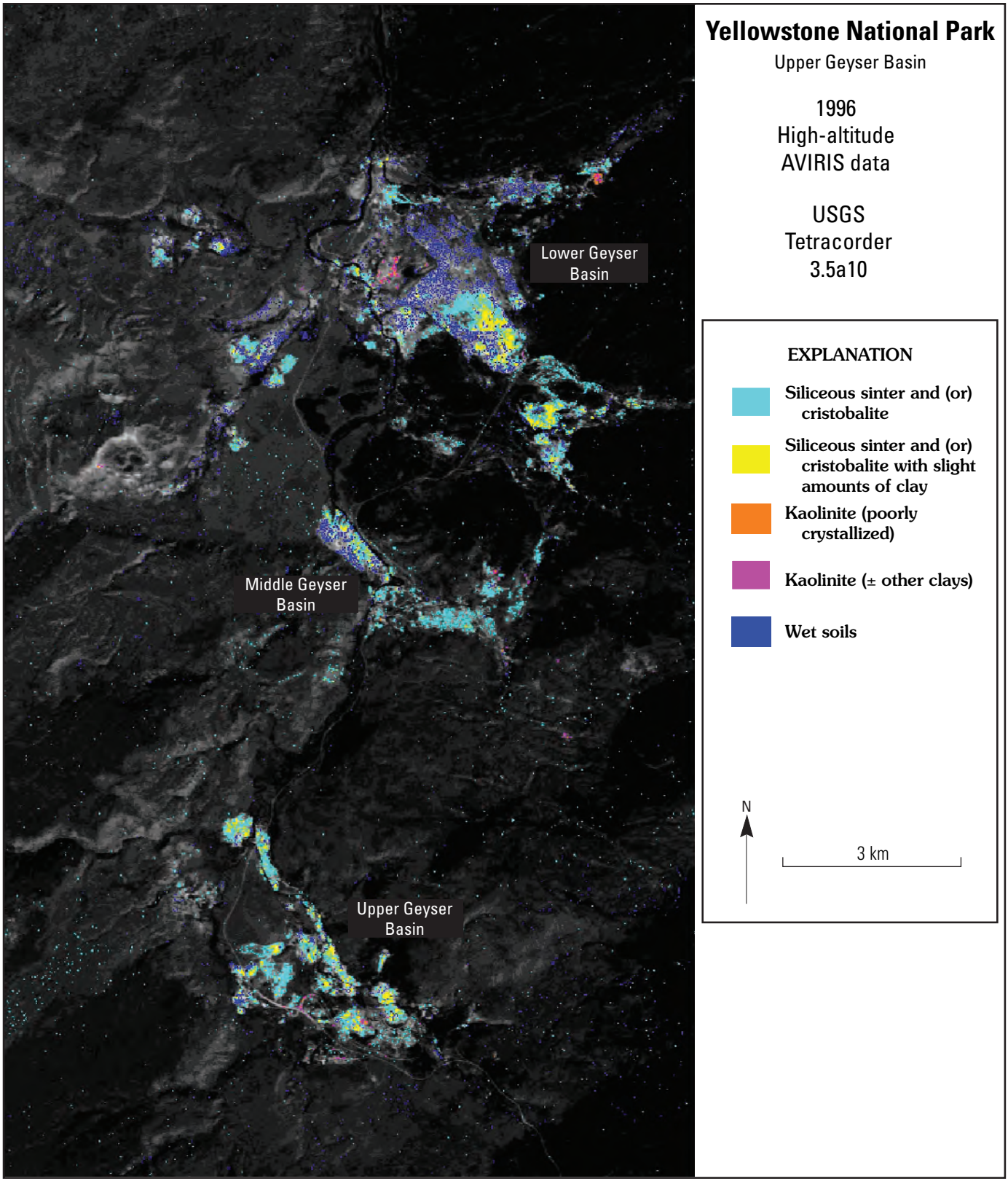

Figure 6. Mineral map of Lower, Midway, and Upper Geyser Basins.

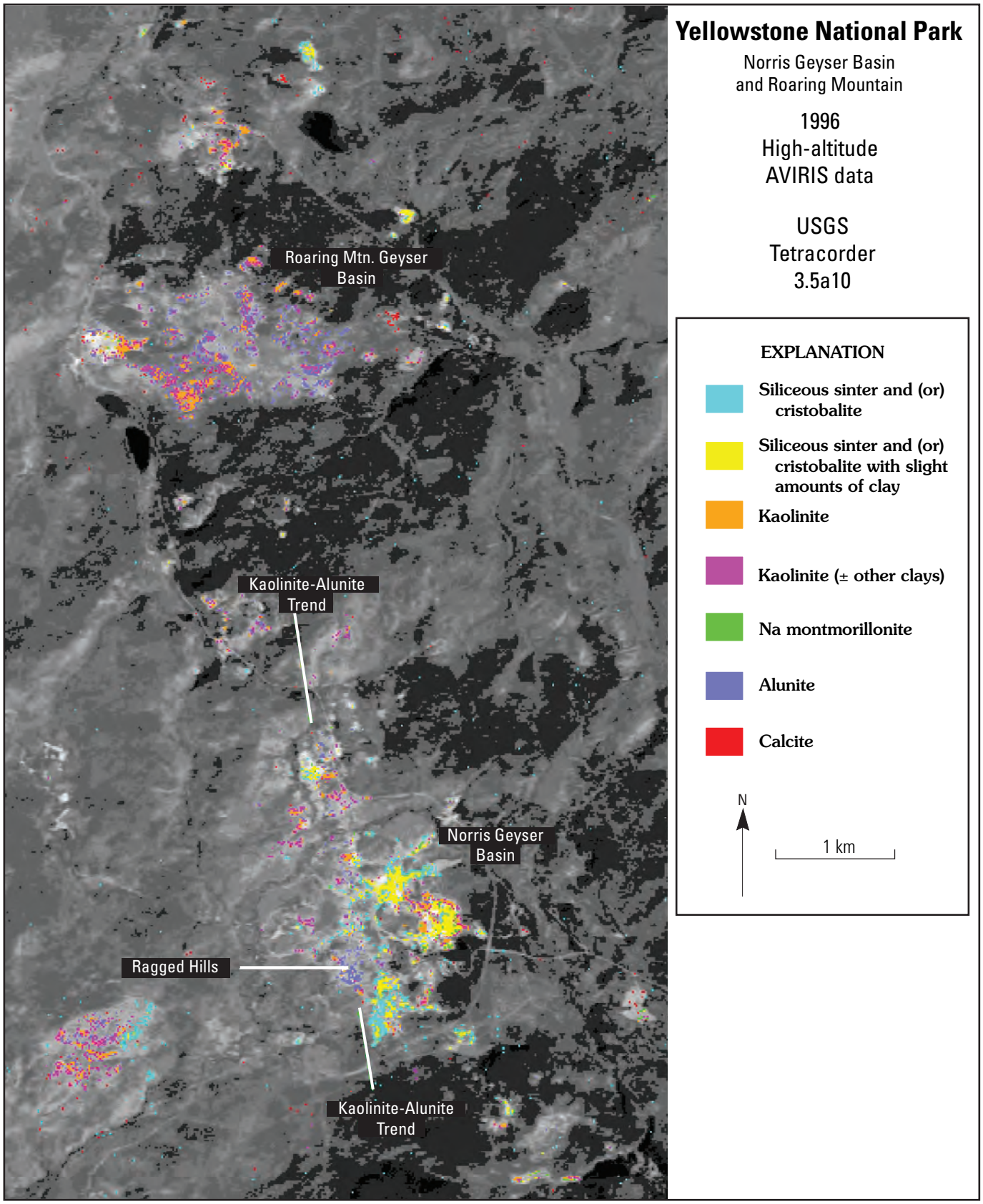

Figure 7. Mineral map of Norris Geyser Basin and Roaring Mountain.

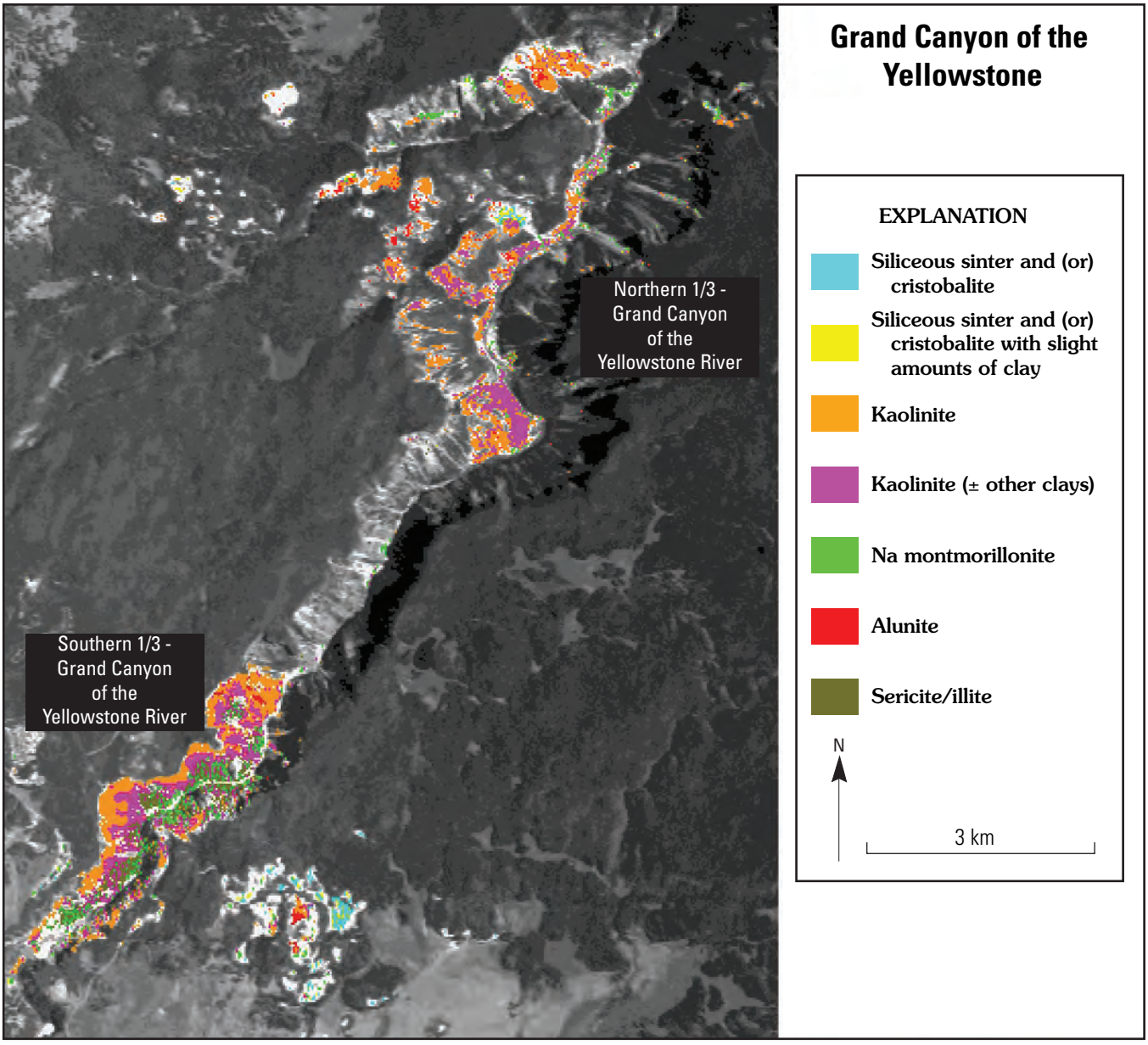

A

Figure 8*A*. Map of sinter, clay minerals, and sulfate minerals of the Grand Canyon of the Yellowstone River.

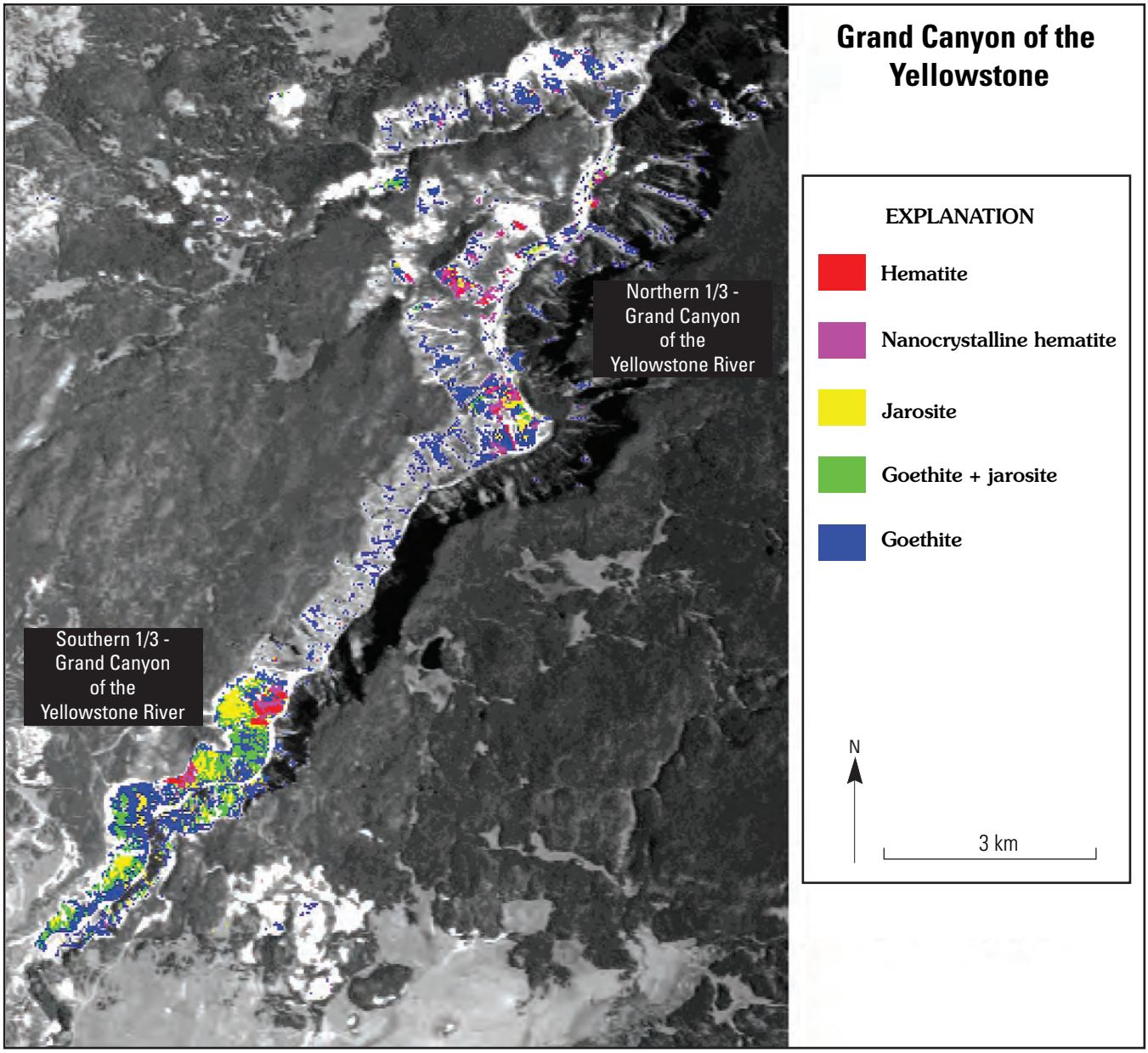

B

Figure 8*B*. Map of iron-bearing minerals of the Grand Canyon of the Yellowstone River.

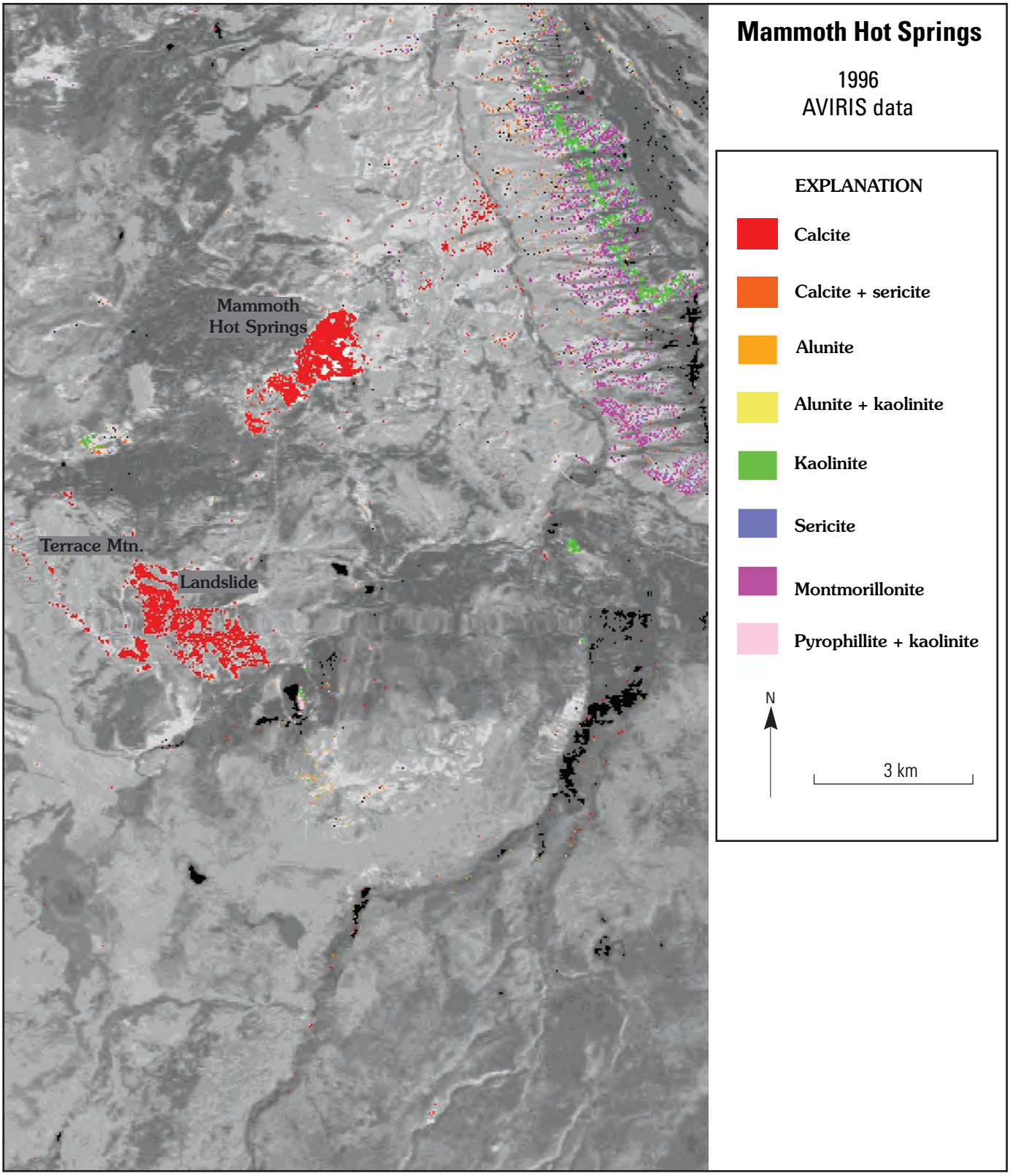

Figure 9. Mineral map of Mammoth Hot Springs.

Mammoth Hot Springs

Mammoth Hot Springs (fig. 9) is a large travertine deposit that was precipitated from water that percolated through underlying limestone bedrock. Mammoth Hot Springs and Terrace Mountain, an inactive travertine deposit to the southwest, have strong carbonate spectral features that map as calcite. Travertine has slid down the southeast side of Terrace Mountain, forming a well-exposed jumble of calcite. Of note is the clean appearance of the travertine; no clay minerals are mapped in the deposits. Kaolinite and alunite are mapped in a small region just west of Mammoth Hot Springs, whereas a variety of clay minerals are mapped across the river, to the northeast, in sedimentary terrain. Travertine deposits are also found north of the Lower Geyser Basin at Terrace Spring and north of Gardner, Mont. (neither area is shown on fig. 9).

Conclusions

Geochemical differences in the types of hydrothermal activity in Yellowstone National Park are inferred from mineral distributions that were mapped using imaging spectrometry. Two main geochemical systems in the basins examined in this study were identified and mapped: (1) abundant neutral-pH chloride-rich water and (2) restricted acid-sulfate water. Abundant neutral-pH chloride-rich water is assumed to have a meteoric (surface-derived) origin, indicated by silica and montmorillonite mapped at Lower and Upper Geyser Basins, Mammoth Hot Springs, and in parts of Norris Geyser Basin. This water is recirculated by convective heating in the geothermal source rock, and it leaches and transports silica and chloride complexes to the surface. Restricted acid-sulfate water is postulated on the basis of the presence of alunite, kaolinite, and jarosite in parts of Norris Geyser Basin, on Roaring Mountain, and in the Grand Canyon of the Yellowstone River. The water is derived mainly from the neutral-pH chloride-rich water; it is enriched in sulfates as a result of near-surface boiling that concentrates steam, H_2S, and CO_2 gases that, in turn, lower the pH of the water and form acid-sulfate minerals.

Geologic structure and wallrock lithology control fluid access to and from geothermal reservoirs and also control the fluid chemistry-wallrock reactions. Carbonate-rich bedrock lithologies yield fluids that are saturated with calcium carbonate, forming travertine terraces. Rhyolite volcanic beds yield fluids that are saturated in silica. Spectral mineral mapping can identify and distinguish both deposit types.

As fluid-channel locations change with time, blocking and unblocking passageways through fluid-leaching action and earthquakes, shifts in fluid chemistry change the compositions of alteration minerals. Overprinting of these alteration minerals is present in most of the areas mapped, suggesting that chemical-compositional changes are active within the hydrothermal systems of Yellowstone National Park.

AVIRIS data has been used to map regional hydrothermal-alteration assemblages in selected areas of Yellowstone National Park. Many of the areas are inaccessible or are in hazardous terrain, thus restricting ground access. Analysis of these data have identified structural trends, and mapped minerals may indicate underlying fluid geochemistry. This study has introduced new questions about the complex mineralogic overprinting that occurs through time.

References Cited

Bargar, K.E., and Beeson, M.H., 1985, Hydrothermal alteration in research drill hole Y-3, Lower Geyser Basin, Yellowstone National Park, Wyoming: U.S. Geological Survey Professional Paper 1054-C, 23 p.

Boardman, J.W., 1997, Mineralogic and geochemical mapping at Virginia City, Nevada, using 1995 AVIRIS data, in Proceedings of the twelfth thematic conference on geological remote sensing, Denver, Colo.: Ann Arbor, Environmental Research Institute of Michigan, p. 21–28.

Boardman, J.W., 1998, Leveraging the high dimensionality of AVIRIS data for improved sub-pixel target unmixing and rejection of false positives—Mixture tuned matched filtering, *in* Summaries of the seventh JPL airborne earth science workshop, v. 1, AVIRIS workshop: Jet Propulsion Laboratory Publication 97-21, 55 p..

Clark, R.N., Gallagher, A.J., and Swayze, G.A., 1990, Material absorption band depth mapping of imaging spectrometer data using a complete band shape least-squares fit with library reference spectra, *in* Proceedings of the second airborne visible/infrared imaging spectrometer (AVIRIS) workshop: Jet Propulsion Laboratory Publication 90-54, p. 176–186.

Clark, R.N., and Swayze, G.A., 1995, Mapping minerals, amorphous materials, environmental materials, vegetation, water, ice and snow, and other materials—The USGS Tricorder algorithm, *in* Green, R.O., ed., Summaries of the fifth annual JPL airborne earth science workshop, January 23–26: Jet Propulsion Laboratory Publication 95-1, p. 39–40.

Clark, R.N., Swayze, G.A., and Gallagher, A.J., 1993, Mapping minerals with imaging spectroscopy, chap. N *of* Scott, R.W., Jr., Detra, P.S., and Berger, B.R., eds., Advances related to United States and international mineral resources—Developing frameworks and exploration technologies: U.S. Geological Survey Bulletin 2039, p. 141–150.

Clark, R.N., Swayze, G.A., Gallagher, A.J., Gorelick, N., and Kruse, F.A., 1991, Mapping with imaging spectrometer data using the complete band shape least-squares algorithm simultaneously fit to multiple spectral features from multiple materials, *in* Proceedings of the third airborne visible/infrared imaging spectrometer (AVIRIS) workshop: Jet Propulsion Laboratory Publication 91-28, p. 2–3.

Clark, R.N., Swayze, G.A., Heidebrecht, K.B., Goetz, A.F.H., and Green, R.O., 1993, Comparison of methods for calibrating AVIRIS data to ground reflectance, *in* Summaries of the fourth annual JPL airborne geosciences workshop, Volume 1: AVIRIS Workshop, Jet Propulsion Laboratory Publication 93-26, p. 31–34.

Clark, R.N., Swayze, G.A., Livo, K.E., Kokaly, R.F., Sutley, S.J., Dalton, J.B., McDougal, R.R., and Gent, C.A., 2003, Imaging spectroscopy—Earth and planetary remote sensing with the USGS Tetracorder and expert systems: Journal of Geophysical Research, v. 108, no. E12, 5131, doi: 10.1029/2002JE001847, 44 p.

Gao, Bo-Cai, Heidebrecht, K.B., and Goetz, A.F.H., 1997, Atmosphere removal program (ATREM) Version 3.0 User's Guide: Boulder, University of Colorado, Center for the Study of Earth From Space, 27 p.

Keith, T.E.C., White, D.E., and Beeson, M.H., 1978, Hydrothermal alteration and self-sealing in Y-7 and Y-8 drill holes in northern part of Upper Geyser Basin, Yellowstone National Park, Wyoming: U.S. Geological Survey Professional Paper 1054-A, 26 p.

Kruse, F.A., 1998, Spectral identification of image end-members determined from AVIRIS data [abs.], *in* Summaries of the seventh JPL airborne earth science workshop, v. 1. AVIRIS workshop: Jet Propulsion Laboratory Publication 97-21, p. 257.

Kruse, F.A., 1999, Mapping hot spring deposits with AVIRIS at Steamboat Springs, Nevada, *in* Summaries of the eighth JPL airborne earth science workshop: Jet Propulsion Laboratory Publication 99-17, p. 239–245.

Kruse, F.A., Huntington, J.H., and Green, R.O., 1996, Results from the 1995 AVIRIS geology group shoot, *in* Proceedings, second international airborne remote sensing conference and exhibition: Ann Arbor, Environmental Research Institute of Michigan, v. I, p. I-211–I-220.

Kruse, F.A., Lefkoff, A.B., and Dietz, J.B., 1993, Expert system-based mineral mapping in northern Death Valley, California/Nevada, using the airborne visible/infrared imaging spectrometer (AVIRIS), *in* Remote Sensing of Environment, special issue on AVIRIS, May–June 1993: Elsevier, v. 44, p. 309–336.

Mosier, D.L., Sato, Takeo, Page, N.J., Singer, D.A., and Berger, B.R., 1986, Descriptive model of Creede epithermal veins, *in* Cox, D.P., and Singer, D.A., eds., Mineral deposit models: U.S. Geological Survey Bulletin 1693, p. 145–149.

Rockwell, B.W., Clark, R.N., Livo, K.E., McDougal, R.R., Kokaly, R.F., and Vance, Sam, 1999, Preliminary materials mapping in the Park City region for the Utah USGS-EPA imaging spectroscopy project using both high and low altitude AVIRIS data, *in* Green, R.O., ed., Summaries of the eighth JPL airborne earth science workshop, Jet Propulsion Laboratory Publication 99-17, p. 365–375.

Smith, R.B., and Braile, L.W., 1993, Topographic signature, space-time evolution, and physical properties of the Yellowstone-Snake River Plain volcanic system—The Yellowstone hotspot, *in* Snoke, A.W., Steidtmann, J.R., and Roberts, S.M., eds., Geology of Wyoming: Geological Survey of Wyoming Memoir 5, p. 694–754.

Thompson, A.J.B., 1991, Acid-sulfate alteration in the Marysvale-Pioche mineral belt—A guide to gold mineralization: Utah Geological and Mineral Survey Miscellaneous Publication 91-2, 29 p.

White, D.E., Fournier, R.O., Muffler, L.J.P., and Truesdell, A.H., 1975, Physical results of research drilling in thermal areas of Yellowstone National Park, Wyoming: U.S. Geological Survey Professional Paper 892, 70 p.

White, D.E., Hutchinson, R.A., and Keith, T.E.C., 1988, The geology and remarkable thermal activity of Norris Geyser Basin, Yellowstone National Park, Wyoming: U.S. Geological Survey Professional Paper 1456, 84 p.